Agronomy Research **17**(2), 481–490, 2019
https://doi.org/10.15159/AR.19.103

Methodology of the stress detemination in the tool module during the work of the agriculture machine

A. Kešner[1,*], R. Chotěborský[1], M. Linda[2] and M. Hromasová[2]

[1]Czech University of Life Sciences Prague, Facult of Engineering, Department of Material Science and Manufacturing Technology, Kamýcká 129, CZ165 21 Prague, Czech Republic
[2]Czech University of Life Sciences Prague, Faculty of Engineering, Department of Eletrical Engineering and Automation, Kamýcká 129, CZ165 21 Prague, Czech Republic
*Correspondence: kesner@tf.czu.cz

Abstract. Machine construction is designed using by mathematical models. The frame is a fundamental part of an agricultural soil cultivation machine so that forces were transfered during transport and machine work to frame. The stress in the machine frame is important to know for the best frame design of the machine. The mathematical model included measued strain can able to design or detect deficiencies on the machine frame. Due to the transfer of forces from the tools, stress is created in the machine frame. High requirements are placed on the determination of boundary conditions for mathematical models in agricultural machinery. Various types, sizes and equipment of agricultural tools significantly affect the transfer of draught force to the machine. The direction and magnitude of the forces, that are caused by agricultural tools, it is important to find out. Ansys mechanical solver have been used to determination strain like response of frame from chisel module. The results can be used as a boundary condition for mathematical models.

Key words: agricultural machine, mathematical model, stress, simulation

INTRODUCTION

The design of an agricultural machine is currently being built using modern technologies such as computer simulation (Kheybari & Salehpour, 2015). When creating a mathematical model it is necessary to know its load on the frame of the agricultural machine (Abo Al-kheer et al., 2011). The transporting and working position of the agricultural machine are important positions when designing the machine. Frames of agricultural machines are stressed from the tool module during working of machine on the field (Ani et al., 2018). Exertion from tool modules causes disturbances such as cracks or deformations on the frame of agricultural machines (Paraforos et al., 2014). Farm machinery manufacturers use the same tool modules for multiple types of machines (the width of the machine, etc.). Stress is an important boundary condition for creating mathematical models of agricultural machinery (Govindarajan & Gnanamoorthy, 2007).

Stress measurement is used for components and machines in many different fields – as residual stresses in production and machining (Sutanto & Madl, 2018), design of

combined agricultural machinery (Bulgakov et al., 2016). Measurement conditions are important for real stress measurement from strain gauges (Lindblom & Cashion, 2005).

During the operation of the agricultural machine, the force tool acts to stress the machine frame (Nurmiev et al., 2018). The forces generated by the tool model are very fast, when the stress is rapidly declining and rising. The soil resistance play an important role (Chotěborský & Linda, 2016). It this reason, why the manufacturers of agricultural machinery report the maximum resistance of the land that the location can have for the work of the machine (Cardei et al., 2018). An obstacle in the soil can cause an immediate increase in strength (Bulgakov et al., 2016). For this reason, the tool modules are protected. Protecting the tool module will allow it to deflect so that the tool module position is deflected when the obstacle impacts. The machine stress is not exceeded by changing the tool module position. The protection is set so that when the maximum machine resistance is reached, the machine's working depth is reduced. Increased stress can not occur on the machine than it is designed on (Bulgakov et al., 2016).

The magnitude of stress from the tool module determines its size and shape (Chotěborský & Linda, 2015). In order to determine the appropriate place on the flexi-tine and the position on the machine frame, it is possible to repeat the measurement for different chisels and coulters and to determine the influence of the tool on the stress (Ahmed et al., 2014).

The main reason for this measurement is to find out the boundary conditions for calculating mathematical models. Mathematical models are part of the design solution for machine design.

The aim of this work was to design a suitable procedure for detecting stress acting on the machine frame from the tool module.

MATERIALS AND METHODS

The workflow consisted of several parts. The first, it was to determine the measuring points in assemble frame and it calibrate the stress measurement devices. It was also the detection of maximum values of strain in the machine frame. Field experiments were carried out subsequently.

Measuring equipment

The stress was measured on the machine frame and the tool module. The device was built for 8 measuring points. Data transfer was performed via WiFi. Critical places were chosen on a mathematical model. The chosen places were grinded before gluing of strain gauges. The strain gauges were silicon resistance type AP130-6-35/BP/Au. The measurement procedure is described in the literature (Furrer & Semiatin S.L., 2009).

$$\varepsilon_M = \frac{-C_1 + \sqrt{C_1^2 + 4 \times C_2 \times \left(1 - \frac{R_{REL}}{R_2}\right)}}{2 \times C_2} \quad (1)$$

where ε_M – deformation on surface [-], C_1 – linear coefficient of deformation equation [-]; C_2 – quadratic coefficient of deformation equation [-], R_2 – semiconductor compensation strain gauge [Ω], R_{REL} – relative strain gauge [Ω].

Fig. 1 shows the location of strain gauges on the machine. The location of the strain gauges was selected according to the mathematical model where the force on the tip of

chisel of the tool modules was loaded. The forces were assume in the x, y, z axes in ratio 1:0.1:0.01 and the strain was determine in a mathematical model. The stain gauge were glued in place with ideal direction of strain in place 1 – 3 and 6 – 8 on frame and 4 and 5 were place on flexi tine.

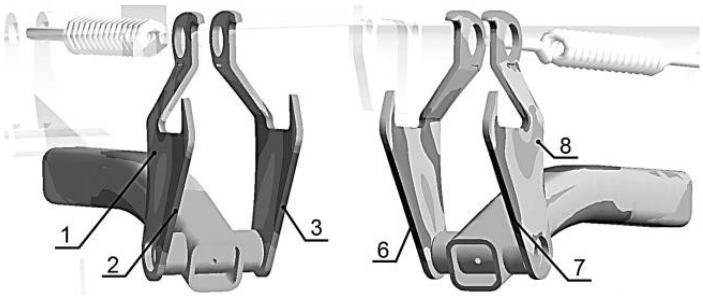

Figure 1. Left – Location of strain gauges 1, 2, 3, to the right the location of strain gauges 6,7,8 on frame of test machine.

Fig. 2 shows a tool module that is fitted with strain gauges. The module thus prepared is ready for installation on the machine.

Figure 2. The tool module is ready for installation on the test machine.

1 module allowed to connect 8 measuring points. The device is powered by an integrated battery. Connectors CAN 9 are used to connect measuring positions. The measuring application was designed to control the module. The application can be used to set the measurement mode, the sequential buffer and the number of channels. Fig. 3 shows the entire connection of the measuring device.

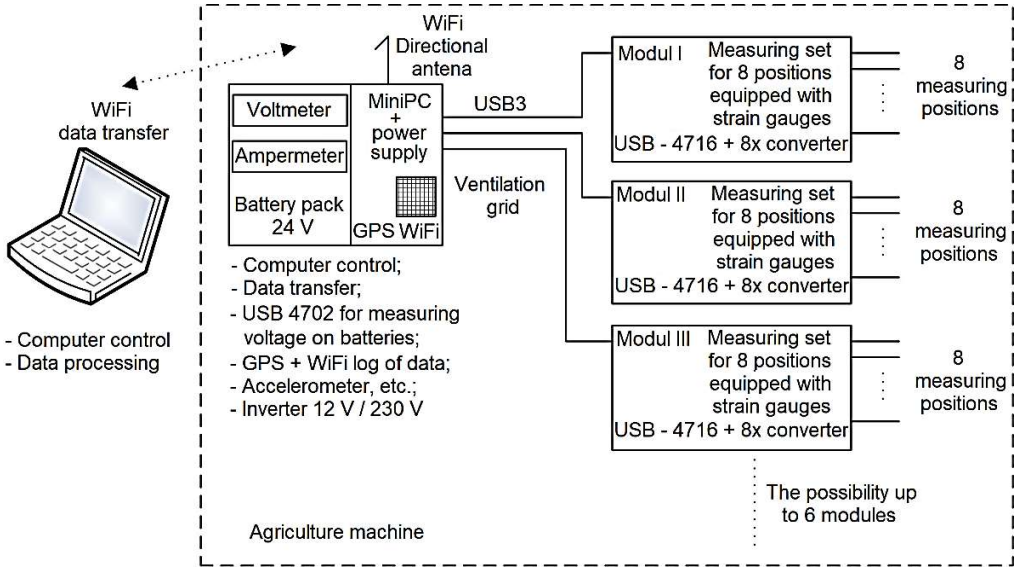

Figure 3. Scheme of a measuring device for recording strain from strain gauges during experimental tests on the field.

Detecting maximum stress values

The type of sandyclay soil is important to follow when designing the machine. It is necessary to determine the limit conditions that may occur during machine operation. These limit conditions have been ensured by the design of an experimental ride with blocked fuse of tool module. These conditions ensure that the maximum load is determined during the experimental ride.

Experimental rides

Two agricultural tools (chisels) were selected for tests. One chisel was fitted with wings, the second was without wings – see Fig. 4.

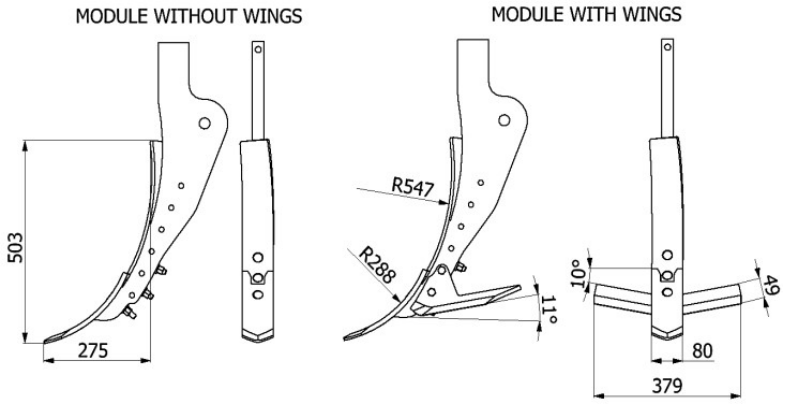

Figure 4. Modules of tools used for tests (in millimetres).

Soil resistance is defined by the module surface – chisels, ridging body and wings. According to Fig. 4 the area module for soil resistance is 40,240 mm^2 (80 mm x 503 mm) and for chisel with wings is area of soil resistance 54,891 mm^2 [80 mm x 503 mm + ((379 mm – 80 mm) x 49 mm)].

The tool modules were installed on a test machine – see Fig. 5.

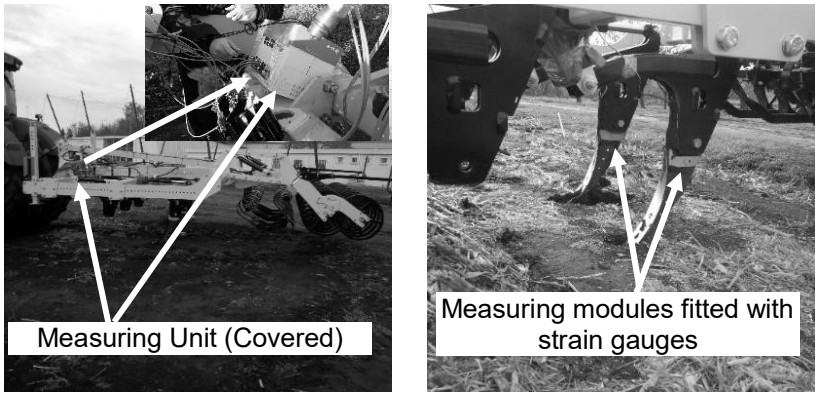

Figure 5. Test machine with installed tool modules for experimental rides – left all machine during work, right detail of module with tools.

The securing was provided by means of hydraulic cylinders for the tool modules. The pressure in the hydraulic cylinders is controlled by a pressure regulator. The pressure

in the hydraulic cylinders for active secure was set at 12 MPa. A pressure of 18 MPa was set to lock the fuse. Two experimental rides were carried out. The first experimental ride was carried out with the active fuse of the flexi-tine. The second experimental ride was performed with blocked fuses. The experimental rides parameters are summarized in Table 1.

Table 1. Setting up and parameters for modules of tools

	1st experimental ride	2nd experimental ride
Type of fuse (-)	hydraulic cylinder	hydraulic cylinder
Pressure in hydraulic cylinder (MPa)	12	18
Fuse of protection module (-)	on	off
Force in hydraulic cylinder (kN)	28.50	42.76
Working depth (m)	0.3	0.3
Area of modulus resistance in soil without wings (m^2)	0.040 24	0.040 24
Area of modulus resistance in soil with wings (m^2)	0.054 981	0.054 981
Working speed ($km \times h^{-1}$)	10.6	10.6
Tractor power (kW)	239	239
Place of measuring (-)	50.127652 14.374566	50.127510 14.374756

The course of the experimental ride was measured from the beginning of the tool's work in the soil of the tool until the tool was finished work in the soil.

The diagram of the connection of the measuring tool module to the machine frame is shown in Fig. 6.

The FEM model was used to determination of boundary condition. Measured strain was response of model and forces and moments were used as variables in parametric modelling in steady state for blocked fuse. Step by step algorithm cycles found a solution which will be under closely to real average strain. The limit was used 10% error. Model of tool module was calculated on Intel® Xeon® Processor CPU E5 - 1650 v3@, processor base frequency 3.50 GHz.

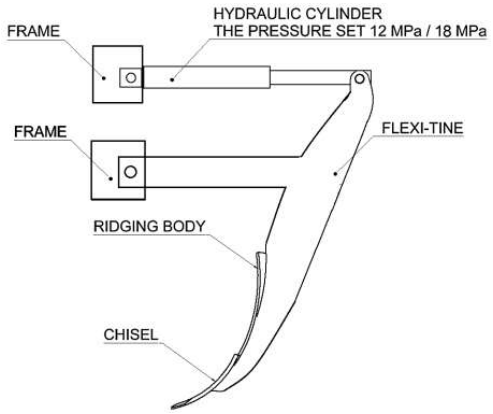

Figure 6. Module mounting diagram – active fuse 12 MPa, blocked fuse 18 MPa.

RESULTS AND DISCUSSION

The time frequency *t* is shown for the beginning work of the tool in soil, the classic machine work in soil, and the finish work of the tool in Figs 7 to 10. The individual distortions ε correspond to the position of the measuring points. The measuring points were selected according to the mathematical model with the prevailing stress in one axis.

The deformation distribution distortion for the experimental ride with the set activared fuse is shown in Figs 7 and 8.

The same course was observed for measuring points 2 and 6 as well as for measuring points 3 and 7.

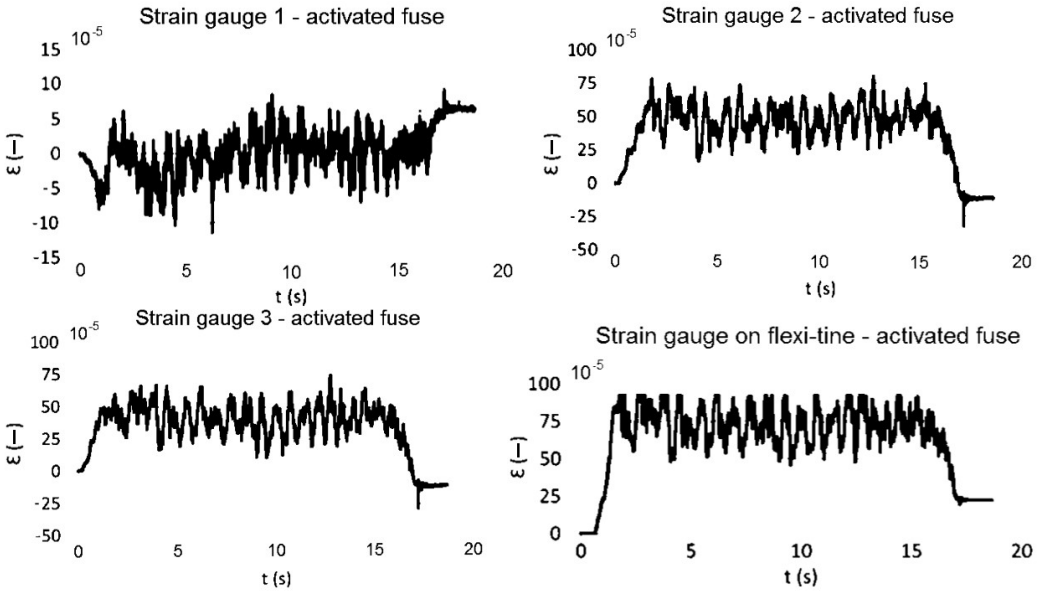

Figure 7. Dependence between deformation ε and time during the experimental ride, tools with wings, active fuse.

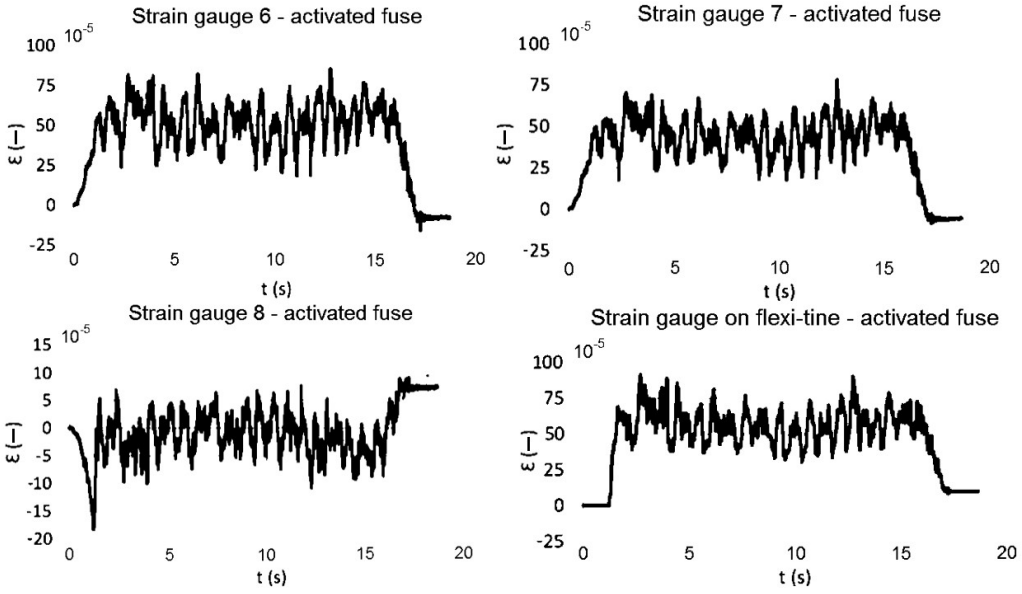

Figure 8. Dependence between deformation ε and time during the experimental ride, tools without wings, active fuse.

The course is clipped for the measuring point in flexo-tine. The reason for this clip is the small measurement range for the strain gauge in flexi-tine. The location of this strain gauge shows large deflections during measurement. The beginning of the tool's work in the soil is value for ε 0 m. Values ε of 0.0005 m to 0.001 m and higher are for

working tool in the soil. For the end of work tool, the value ε again drops to 0 m. This fact was also found for the same measuring point for the second experimental ride.

The deformation distribution distortion for the experimental ride with the set blocked fuse is shown in Figs 9 and 10.

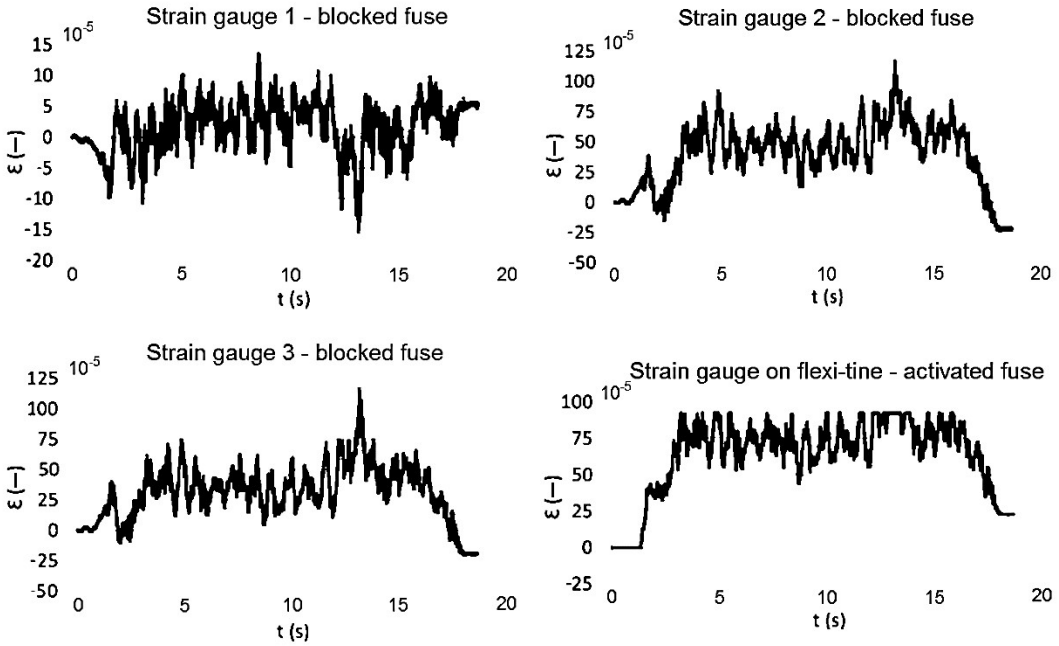

Figure 9. Dependence between deformation ε and time during the experimental ride, tools with wings, blocked fuse.

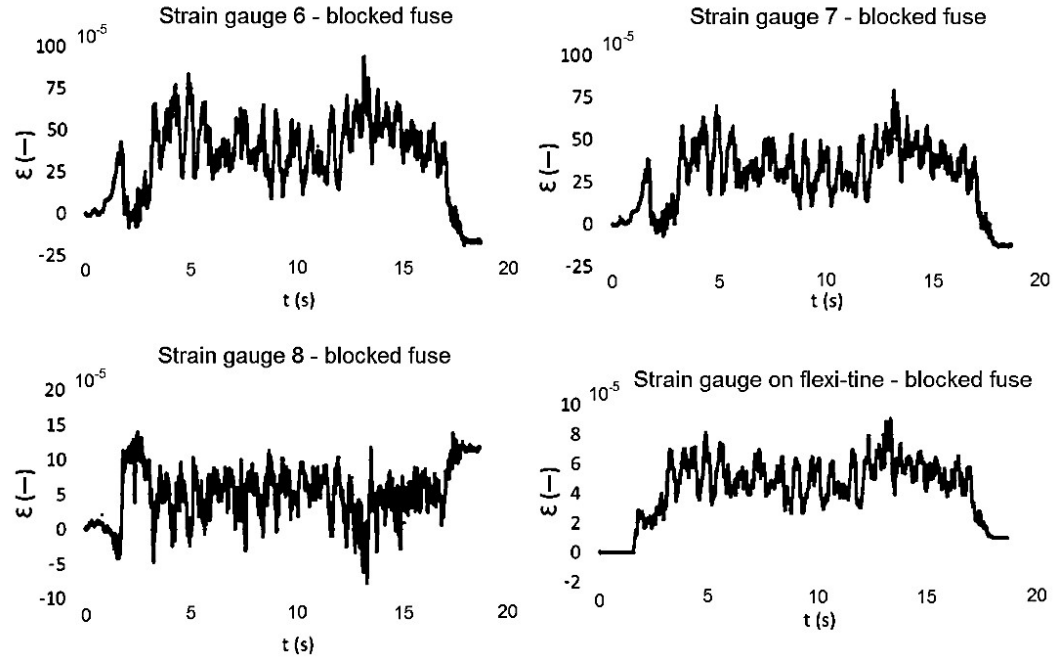

Figure 10. Dependence between deformation ε and time during the experimental ride, tools without wings, blocked fuse.

The measurement courses are similar for measuring points 1 and 8 for 3 and 7. Measurement courses show the same magnitude of deformation ε for measuring points 2 and 6 and 3 and 7.

Large amplitude was detected for blocked fuse for both fixed-tine in 13 second. Machine crossing over an obstacle in the ground (stone) or compressed part of the soil may be the reason for the occurrence of large amplitudes. The opposite direction of the amplitude was found for measurement points 1 and 8. The reason is the opposite orientation of the forces in the measuring point.

Large differences of course were found for the characteristics of experimental rides between activated fuse and blocked fuse. The activated fuse eliminates the force transfer to the frame more than the blocked fuse. All strain is transmitted to the machine frame for blocked fuse.

The chisel with wing has a 26.7% higher area than the wingless chisel. Comparison of strain gauges located at the same locations (1 and 8, 2 and 6, 3 and 7) shown a resuts where it seem higher draght force but lower moment around vertical axis.The courses were analyzed from experimental rides. The entire course was recorded for each experimental ride. The course was divided into parts. The first course was always the beginning of the tool's work in the soil – the time before the tool reached the required working depth – marked by t_1 in Fig. 11. The work of the tool in the soil is recorded by t_2 for the required working depth. The end of working for tool is recorded at t_3. The period t_4 shows the increase in resistance for the tool while working at the standard depth.

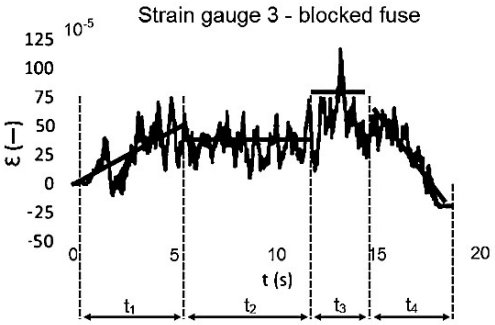

Figure 11. Dependence between deformation ε and time during experimental ride, without wings, blocked fuse.

The direction, magnitude of the acting force in the x, y, z axes of the tool module is a necessary boundary condition for the construction of mathematical models. Measured data were used for a parametric computation of frame part in FEM. Final parametric cycle of steady state FEM algorithm for mean strain during t_2 shown an acceptable boundary condition which are presented in Table 2. Results shown higher draught force for wings chisel and also higher stability in x-axis determined lateral forces and lower moment in tool module.

Table 2. Boundary conditions for steady state during field tests

	Fx (N]	Fy (N)	Fz (N)	Mx (Nm)	My (Nm)	Mz (Nm)
module with wings	2 553	-36,334	-291	139	70	4,871
modelu without wings	1,642	-42,567	-5,690	78	74	4,482

Many authors are concerned with detecting traction resistance in agricultural machinery. No literature has been found that deals directly with strain measurements.

(Kumar et al., 2016) work is concerned with detecting the traction resistance of an agricultural machine using its own developed digital system. Their results make it

possible to optimize tractor consumption. The tractor's consumption depends on the size of the traction resistance of the agricultural machine. In this work, the traction resistance can also be calculated based on the measured courses. The fuel consumption of the tractor and other quantities can be calculated from the traction resistance in this work.

The influence of plow angles in dependence on traction resistance was studied in (McKyes & Desir, 1984). The impact of tool resistance with wings and tool without wings has been investigated in this work. The ratio of areas correspond with ratio of strain. Significant impact of the wings was detected on the resistance of the tool module.

(Onwualu, 1998) examined the influence of velocity on traction resistance. A constant speed was used in this work. The design of the test runs identified the maximum traction resistance that can be developed on the machine frame. Different speeds can be neglected due to the size of the traction resistance.

CONCLUSIONS

A method was developed to measure the stress on the frame of the agricultural machine. Stress is generated from the tool module in the machine frame. The magnitude of stress is one of the marginal conditions for creating a mathematical model design.

Depending on the models and measured stress, the geometry of the tool can be modified.

The maximum traction resistance was determined by the fuse protection system. For this reason, the type of soil was not detected. Soil served only as a load for experimental drives.

The effect of the tool module resistance has been detected. The effect is shown in the course for wing and without modules.

The effects of the tool modules can be detected for different sizes and shapes by the procedure described in this paper. The procedure can be used, for example, for disk machines. However, the discs are affected by the momentum created by angled disk operation.

From the measurements used in this work, more data can be calculated such as traction resistance, tractor fuel consumption, resistance in various work dumps, effect of tool size and shape, etc.

REFERENCES

Abo Al-kheer, A., Eid, M., Aoues, Y., El-Hami, A., Kharmanda, M.G. & Mouazen, A.M. 2011, Theoretical analysis of the spatial variability in tillage forces for fatigue analysis of tillage machines. *Journal of Terramechanics* **48**(4), 285–295.

Ahmed, S.F., Zein Eldin, A.M. & Abdulaal, S.M. 2014. Reducing draft required for a simple chisel tool. *AMA, Agricultural Mechanization in Asia, Africa and Latin America* **45**(4), 26–31.

Ani, O.A., Uzoejinwa, B.B., Ezeama, A.O., Onwualu, A.P., Ugwu, S.N. & Ohagwu, C.J. 2018. Overview of soil-machine interaction studies in soil bins. *Soil and Tillage Research* **175**, 13–27.

Bulgakov, V., Adamchuk, V., Arak, M., Nadykto, V., Kyurchev, V. & Olt, J. 2016, Theory of vertical oscillations and dynamic stability of combined tractor-implement unit. *Agronomy Research* **14**(3), 689–710.

Cardei, P., Vladutoiu, L., Chisiu, G., Tudor, A., Sorica, C., Gheres, M. & Muraru, S. 2018. Research on friction influence on the working process of agricultural machines for soil tillage. *IOP Conference Series: Materials Science and Engineering* **444**.

Chotěborský, R. & Linda, M. 2015. FEM based numerical simulation for heat treatment of the agricultural tools. *Agronomy Research* **13**(3), 629–638.

Chotěborský, R. & Linda, M. 2016. Determination of chemical content of soil particle for abrasive wear test. *Agronomy Research* **14**, 975–983.

Furrer, D. & Semiatin, S.L. 2009. ASM Handbook Volume 22A: Fundamentals of Modeling for Metals Processing. *ASM International*, 284–325.

Govindarajan, N. & Gnanamoorthy, R. 2007. Rolling/sliding contact fatigue life prediction of sintered and hardened steels. *Wear* **262**(1–2), 70–78.

Kheybari, S. & Salehpour, R. 2015. The optimization of the paddy field irrigation scheduling using mathematical programming. *Water Science and Technology: Water Supply* **15**(5), 1048–1060.

Kumar, A.A., Tewari, V.K. & Nare, B. 2016. Embedded digital draft force and wheel slip indicator for tillage research. *Computers and Electronics in Agriculture* **127**, 38–49.

Lindblom, G.P. & Cashion, B.S. 2005, Operational considerations for optimum deposition efficiency in aerial application of dispersants. In *2005 International Oil Spill Conference, IOSC 2005,* pp. 5923.

McKyes, E. & Desir, F.L. 1984. Prediction and field measurements of tillage tool draft forces and efficiency in cohesive soils. *Soil and Tillage Research* **4**(5), 459–470.

Nurmiev, A., Khafizov, C., Khafizov, R. & Ziganshin, B. 2018. Optimization of main parameters of tractor working with soil-processing implement. *Engineering for Rural Development* **17**, 161–167.

Onwualu, A. 1998. Draught and vertical forces obtained from dynamic soil cutting by plane tillage tools. *Soil and Tillage Research* **48**(4), 239–253.

Paraforos, D.S., Griepentrog, H.W., Vougioukas, S.G. & Kortenbruck, D. 2014, Fatigue life assessment of a four-rotor swather based on rainflow cycle counting. *Biosystems Engineering* **127**, 1–10.

Sutanto, H. & Madl, J. 2018, Residual stress development in hard machining - a review. *IOP Conference Series: Materials Science and Engineering* **420**, 012031.